

The relativistic jet and its central engine of *Fermi* blazars

HUBING XIAO,¹ ZHIHAO OUYANG,² LIXIA ZHANG,^{3,4,5} LIPING FU,¹ SHAOHUA ZHANG,¹ XIANGTAO ZENG,^{3,4,5} AND JUNHUI FAN^{3,4,5}

¹*Shanghai Key Lab for Astrophysics, Shanghai Normal University
Shanghai, 200234, China*

²*School of Physics and Materials Science, Guangzhou University
Guangzhou, 510006, China*

³*Center for Astrophysics, Guangzhou University
Guangzhou, 510006, China*

⁴*Key Laboratory for Astronomical Observation and Technology of Guangzhou
Guangzhou 510006, China*

⁵*Astronomy Science and Technology Research Laboratory of Department of Education of Guangdong Province
Guangzhou, 510006, China*

ABSTRACT

Jet origination is one of the most important questions of AGN, yet it stays obscure. In this work, we made use of information of emission lines, spectral energy distributions (SEDs), *Fermi*-LAT γ -ray emission, construct a blazar sample that contains 667 sources. We notice that jet power originations are different for BL Lacs and for FSRQs. The correlation between jet power P_{jet} and the normalized disk luminosity $L_{\text{Disk}}/L_{\text{Edd}}$ shows a slope of -1.77 for BL Lacs and a slope of 1.16 for FSRQs. The results seems to suggest that BL Lac jets are powered by extracting blackhole rotation energy, while FSRQ jets are mostly powered by accretion disks. Meanwhile, we find the accretion ratio $\dot{M}/\dot{M}_{\text{Edd}}$ increase with the normalized γ -ray luminosity. Base on this, we propose a dividing line, $\log(L_{\text{BLR}}/L_{\text{Edd}}) = 0.25 \log(L_{\gamma}/L_{\text{Edd}}) - 2.23$, to separate FSRQs and BL Lacs in the diagram of $L_{\text{BLR}}/L_{\text{Edd}}$ against $L_{\gamma}/L_{\text{Edd}}$ through using the machine learning method, the method gives an accuracy of 84.5%.

In addition, we propose an empirical formula, $M_{\text{BH}}/M_{\odot} \simeq L_{\gamma}^{0.65}/21.46$, to estimate blackhole mass based on a strong correlation between γ -ray luminosity and blackhole mass. Strong γ -ray emission is typical in blazars, and the emission is always boosted by a Doppler beaming effect. In this work, we generate a new method to estimate a lower-limit of Doppler factor δ and give $\delta_{\text{BL Lac}} = 7.94$ and $\delta_{\text{FSRQ}} = 11.55$.

1. INTRODUCTION

Active galactic nuclei (AGNs) are the most energetic and persistent extragalactic objects in the universe. Blazars exhibit extreme observation properties, including rapid and high amplitude variability, high and variable polarization, strong and variable γ -ray emissions, or apparent superluminal motions, etc (Wills et al. 1992; Urry & Padovani 1995; Fan 2002; Fan et al. 2004; Kellermann et al. 2004; Rani et al. 2013; Fan et al. 2014; Lyutikov & Kravchenko 2017; Xiao et al. 2019). The extreme observational properties result from Doppler beaming effect caused by relativistic jets (Xiao et al. 2015; Pei et al. 2016; Fan et al. 2017).

Blazars, typically, are hosted by elliptically galaxies and powered by the central supermassive black holes (Urry et al. 2000; Shaw et al. 2012). The broadband spectral energy distribution (SED) of blazar forms a two-hump structure, which the lower energy bump is explained by the synchrotron mechanism and the higher energy bump is attributed to the inverse Compton (IC) scattering in a leptonic scenario.

There are two subclasses of blazars that are characterized based on the emission line strength of optical spectra, namely BL Lacertae objects (BL Lacs) and flat-spectrum radio quasars (FSRQs). The former one characterizes

a spectrum with no or weak emission lines (rest-frame equivalent width, $EW < 5\text{\AA}$), while the latter one shows strong emission line features of $EW \geq 5\text{\AA}$ (Urry & Padovani 1995; Scarpa & Falomo 1997). However, an arbitrary classification base on EW is inadequate. On one hand, a Doppler boosted non-thermal continuum could swamp out spectral emission lines (Blandford & Rees 1978; Xiong & Zhang 2014). On the other hand, EW greater than 5\AA may be the result of a particular low-state of jet activity. Other indicators have been proposed to divide blazars into subclasses. Ghisellini et al. (2011) and Sbarrato et al. (2012) suggested a distinction of accretion ratio based on the luminosity of broad-line region (BLR) measured in Eddington units, $L_{\text{BLR}}/L_{\text{Edd}} \sim 10^{-3}$ or $L_{\text{BLR}}/L_{\text{Edd}} \sim 5 \times 10^{-4}$, to separate FSRQs and BL Lacs. Abdo et al. (2010a) and Fan et al. (2016) used synchrotron peak frequency ($\log \nu_s$) to divide blazars into low-synchrotron-peaked blazars (LSP), intermediate-synchrotron-peaked blazars (ISP) and high-synchrotron-peaked blazars (HSP) and got compatible results of separating boundaries.

Emission lines with half-maximum-full-width (FWHM) greater than 1000 km/s are called broad emission lines, otherwise, narrow emission lines. The broad emission lines are employed to estimate the central blackhole (BH) mass (M_{BH}) by using BLR distance and FWHM assuming the BLR clouds being gravitationally bound by the central BH. The BLR distance can be interpreted through an empirical relation between BLR distance and ionizing luminosity or through reverberation mapping (Wandel et al. 1999; Kaspi et al. 2000, 2005). The reverberation mapping method, requires continuous observations on both continuum and emission line variations, gives a more accurate BLR distance than distance-luminosity correlation. Kaspi et al. (2000) calibrated empirical distance-luminosity correlation by using a reverberation-mapped sample and got $R_{\text{BLR}} \propto L_{5100}^{0.7}$, here L_{5100} is the continuum luminosity at $\lambda = 5100\text{\AA}$. Greene & Ho (2005) noticed that the emission line luminosities of $\text{H}\alpha$ and $\text{H}\beta$ have a strong correlation with L_{5100} . They substituted the L_{5100} with $L_{\text{H}\alpha}$ and $L_{\text{H}\beta}$, and suggested $M_{\text{BH}} \propto L_{\text{H}\alpha}^{0.55}$ and $M_{\text{BH}} \propto L_{\text{H}\beta}^{0.56}$. MgII , CIV were also explored by other researchers (McLure & Dunlop 2004; Vestergaard & Peterson 2006; Vestergaard & Osmer 2009; Shen et al. 2011; Shaw et al. 2012). For some sources without broad emission lines, especially BL Lac objects, their M_{BH} can be estimated from the properties of their host galaxies with $M_{\text{BH}} - \sigma_*$ and $M_{\text{BH}} - L$, where σ_* and L are the stellar velocity dispersion and the bulge luminosity (Woo & Urry 2002; Sbarrato et al. 2012; Xiong & Zhang 2014).

The luminosity of broad line region (L_{BLR}) derived from broad emission lines (Francis et al. 1991; Celotti et al. 1997; Sbarrato et al. 2012), is a good estimator of the power of accretion disk, $L_{\text{Disk}} \simeq 10L_{\text{BLR}}$ (Calderone et al. 2013). Because the emission lines are produced by gas that is photoionized by the disk emission. Thanks to *Fermi*-LAT, we have come to a new era of blazar research. *Fermi* collaboration has released four generations of γ -ray source catalogues. The fourth one (4FGL) contains 5064 sources above 4σ significance, among these sources more than 3130 of identified or associated sources are active galaxies of blazar class (including uncertain type blazars, BCUs.) (Abdollahi et al. 2020). Blazars are strong γ -ray emitters, their γ -ray emissions dominate bolometric luminosity ($L_{\text{jet}}^{\text{bol}}$) of jets. Thus, the L_γ often take the place of $L_{\text{jet}}^{\text{bol}}$ in previous research (Ghisellini et al. 2014; Xiong & Zhang 2014; Zhang et al. 2020). The relativistic jets transport energy and momentum from AGN to large scales, but the jet formation remains unclear. The current theoretical models consider that jet originated either from the accretion disk and powered by accretion or from the central BH and powered by extracting rotation energy (Blandford & Znajek 1977; Blandford & Payne 1982).

The connection between relativistic jet and accretion disk through study γ -ray luminosity, broad emission line, and blackhole mass has been explored by many authors. Sbarrato et al. (2012) studied the blazars that have been detected by *Fermi*-LAT and that are present in the Sloan Digital Sky Survey (SDSS), suggested the L_{BLR} correlates well with L_γ . The correlation proves the emission-line photons to play a role in producing high-energy γ -rays and points out a clue of the relation between accretion ratio and jet power. The correlations between intrinsic γ -ray luminosity and BH mass, Eddington ratio, broad-line luminosity were studied by Xiong & Zhang (2014) and Zhang et al. (2020), and they all show positive correlations. A correlation of $\log L_{\text{BLR}} \sim (0.98 \pm 0.07)\log P_{\text{jet}}$ suggest that jets are powered by extraction from both accretion and BH spin Xiong & Zhang (2014).

In this work, we focus on the study of the correlations between γ -ray emission and BH mass, relativistic jet related quantities to investigate the jet origination and accretion rate of blazars.

This paper is arranged as follows: in Section 2, we present the samples; the data reduction and results are presented in Section 3; Section 4 will be our discussion; our conclusion will be presented in Section 5. The cosmological parameters $H_0 = 73 \text{ km} \cdot \text{s}^{-1} \cdot \text{Mpc}^{-1}$, $\Omega_m = 0.3$ and $\Omega_\Lambda = 0.7$ have been adopted through this paper.

2. THE SAMPLES

We collect broad emission line profiles and BH mass from Paliya et al. (2021), which contains 674 sources. Besides, 10 sources with emission line parameters or BH mass values from literature (Baldwin et al. 1981; Chen et al. 2015) were included by Paliya et al. (2021), and these sources are also employed in our work. The classification of *Fermi* sources are sometimes changed after a new data release. According to the latest classification, there were 17 sources were excluded from the blazar class, finally make us a sample of 667 sources (56 BCUs, 52 BL Lacs and 559 FSRQs). Meanwhile, we collect the γ -ray flux from 4FGL for the sources in our sample. At last, we cross-correlate the sample with Nemmen et al. (2012); Ghisellini et al. (2014); Tan et al. (2020) to get the entire jet power (P_{jet}), the non-thermal radiation power (P_{rad}), and the accretion disk luminosity (L_{Disk}).

2.1. γ -ray luminosity

The SED of blazar is characterized by two broad bumps, peaking in the mm-UV and the MeV-GeV γ -ray bands separately. The emission of the high energy bump is usually the dominant component for blazars, so-called a higher Compton dominance that is quantified by $L_{\text{IC}}/L_{\text{syn}}$, except for some low power BL Lacs. Thus, the γ -ray luminosity is believed to be a representative of blazar non-thermal bolometric luminosity (Ghisellini et al. 2014; Xiong & Zhang 2014; Zhang et al. 2020). An isotropic γ -ray luminosity is expressed as

$$L_{\gamma} = 4\pi d_L^2 (1+z)^{\alpha_{\text{ph}}-2} F, \quad (1)$$

where $d_L = (1+z) \cdot \frac{c}{H_0} \cdot \int_1^{1+z} \frac{1}{\sqrt{\Omega_M x^3 + 1 - \Omega_M}} dx$, z is redshift, $(1+z)^{\alpha_{\text{ph}}-2}$ represents a K -correction, α_{ph} is the γ -ray photon index, and F is the γ -ray flux in units of $\text{erg} \cdot \text{cm}^{-2} \cdot \text{s}^{-1}$. We calculated L_{γ} for these 637 sources, which with available redshift from the NASA/IPAC Extragalactic Database (NED), via Eq.1. The redshift, 4FGL γ -ray photon density and photon spectral index that are listed in columns (3), (4) and (6) of Table 1.

2.2. BH mass and BLR luminosity

Paliya et al. (2021) obtained emission line ($\text{H}\alpha$, $\text{H}\beta$, Mg II , and C IV) luminosity and corresponding continuum luminosity by analyzing optical spectra from SDSS-DR16 data. Continuum luminosity L_{λ} at 5100 Å is estimated from $\text{H}\beta$ luminosity, at 3000 Å is estimated from Mg II luminosity, and at 1350 Å is estimated from C IV luminosity via empirical relations. Then, a virial M_{BH} is estimated through empirical formula

$$\log M_{\text{BH}} = a + b \log L_{\lambda} + 2 \log FWHM, \quad (2)$$

where M_{BH} in units of solar mass M_{\odot} , L_{λ} in units of $10^{44} \text{ erg} \cdot \text{cm}^{-2} \cdot \text{s}^{-1}$, $FWHM$ in units of $\text{km} \cdot \text{s}^{-1}$, and the calibration coefficients a and b are taken from McLure & Dunlop (2004); Vestergaard & Peterson (2006); Shen et al. (2011). The BH mass are listed in column (11) of Table 1.

Moreover, one can infer the luminosity of the entire broad emission line region (L_{BLR}) from emission line luminosity. Celotti et al. (1997) calculated L_{BLR} by scaling strong emission lines to the quasar template spectrum of Francis et al. (1991). They set $\text{Ly}\alpha$ as a reference flux that contributed to 100, the relative weight of $\text{H}\alpha$, $\text{H}\beta$, MgII and C IV lines to 77, 22, 34, and 63, and total broad line flux was fixed at 556. The BLR luminosity is, then, expressed as

$$L_{\text{BLR}} = \sum_i L_i \cdot \frac{\langle L_{\text{BLR, rel}} \rangle}{\sum_i L_{i, \text{rel}}}, \quad (3)$$

where $\langle L_{\text{BLR, rel}} \rangle = 556$, L_i is observed line luminosity, and $L_{i, \text{rel}}$ is relative line luminosity.

2.3. Jet power

The entire power of jet (P_{jet}) generally contains two parts of energy, namely radiation power (P_{rad}) and kinetic power (P_{kin}), that in charge of its non-thermal radiation and its propagation.

There are methods to estimate P_{kin} , P_{rad} , and P_{jet} . Cavagnolo et al. (2010) searched for X-ray cavities in different systems including giant elliptical galaxies and cD galaxies and estimated the required jet power that is able to inflate these cavities or bubbles, obtaining a correlation between ‘cavity’ power and radio luminosity

$$P_{\text{cav}} \approx 5.8 \times 10^{43} \left(\frac{P_{\text{radio}}}{10^{40} \text{ erg} \cdot \text{s}^{-1}} \right)^{0.7} \text{ erg} \cdot \text{s}^{-1}, \quad (4)$$

and assuming $P_{\text{kin}} = P_{\text{cav}}$. The radiation power is expressed as

$$P_{\text{rad}} = 2f \frac{\Gamma^2 L_{\text{jet}}^{\text{bol}}}{\delta^4}, \quad (5)$$

where the factor 2 counts for two-sided jets, f equals 16/5 for the case of radiation power consuming through SSC process. For the case of EC process, $f = 4/3$ and replace δ^4 with $\delta^4(\delta/\Gamma)^2$. Two assumptions, $L_{\text{bol}}^{\text{jet}}$ is represented by L_γ and $\Gamma = \delta$, are both hold for blazars (Ghisellini & Tavecchio 2010; Ghisellini et al. 2014; Xiong & Zhang 2014; Zhang et al. 2020).

The P_{rad} and P_{jet} are obtainable through broadband SED fitting. Assuming that the jet power is carried by relativistic electron, cold proton, magnetic field, and radiation. The jet power is expressed as

$$P_{\text{jet}} = \sum_i \pi R^2 \Gamma^2 c U_i, \quad (6)$$

where $U_i (i = e, p, B, rad)$ are the energy densities associated with the emitting electron U_e , cold proton U_p , magnetic field U_B , and radiation U_{rad} measured in the comoving frame (Ghisellini & Tavecchio 2010; Tan et al. 2020). We collect P_{rad} and P_{jet} from Ghisellini et al. (2014) and Tan et al. (2020) for our sources and list them in columns (4) and (5) of Table 2.

3. RESULTS

3.1. The distributions

The redshift and BH mass distributions of various classes of sources are shown in Fig. 1. The redshift, which are obtained by checking their associate names (from 4FGL) in the NED, distributes from 0.00085 to 6.443 with a mean value of 1.147 ± 0.688 for all the blazars in our sample. The mean redshifts for FSRQs is 1.178 ± 0.652 , for BL Lacs is 0.697 ± 0.479 (4FGL J0823.3+2224 is excluded for the extremely high redshift 6.443), and for BCUs is 1.144 ± 0.698 . The BH mass ranges from 6.35 to 10.2 with a mean value of 8.50 ± 0.58 for all the blazars in our sample. The mean BH masses for FSRQs is 8.56 ± 0.55 , for BL Lacs is 8.18 ± 0.66 , and for BCUs is 8.19 ± 0.57 .

3.2. Correlation between γ -ray luminosity and BH mass

Fig 2 shows BH mass as a function of γ -ray luminosity. We have three sources with debatable γ -ray luminosity due to their redshift, these sources are not shown in Fig 2 and the luminosity of these three sources will not be employed during our analysis through this paper. Two (4FGL J1434.2+4204 and 4FGL J2134.2-0154) of them with at least two order of magnitude lower γ -ray luminosity ($\log L_\gamma = 39.92$ and $\log L_\gamma = 40.38$ in unit of erg/s) than the rest of the sources due to their extreme small redshifts (0.0031 and 0.00085) with respect to the average value of their class in our sample. In addition, we also remove the BL Lac object, 4FGL J0823.3+2224 (OJ 233), for its extremely large and suspicious redshift $z=6.443$. We suspect the redshift of these three sources are mis-estimated for two possible reasons (1) optical counterparts are wrongly associated; (2) or very weak emission lines on the spectrum. Linear regression is applied to analyse the correlation between γ -ray luminosity and BH mass for all the sources in our sample except for the above-mentioned three. The result indicates that BH mass and γ -ray luminosity has a strong correlation from a ordinary least squares (OLS) bisector regression

$$\log \frac{M_{\text{BH}}}{M_\odot} = (0.65 \pm 0.02) \log L_\gamma - (21.46 \pm 1.04),$$

and the correlation coefficient $r = 0.52$ and the chance probability $p = 1.3 \times 10^{-44}$ are obtained through Pearson analysis. The result suggests a strong correlation between BH mass and γ -ray luminosity. Thus we suggest that γ -ray luminosity is a good BH mass estimator of blazar and propose this formula

$$\frac{M_{\text{BH}}}{M_\odot} \simeq \frac{L_\gamma^{0.65}}{21.46}.$$

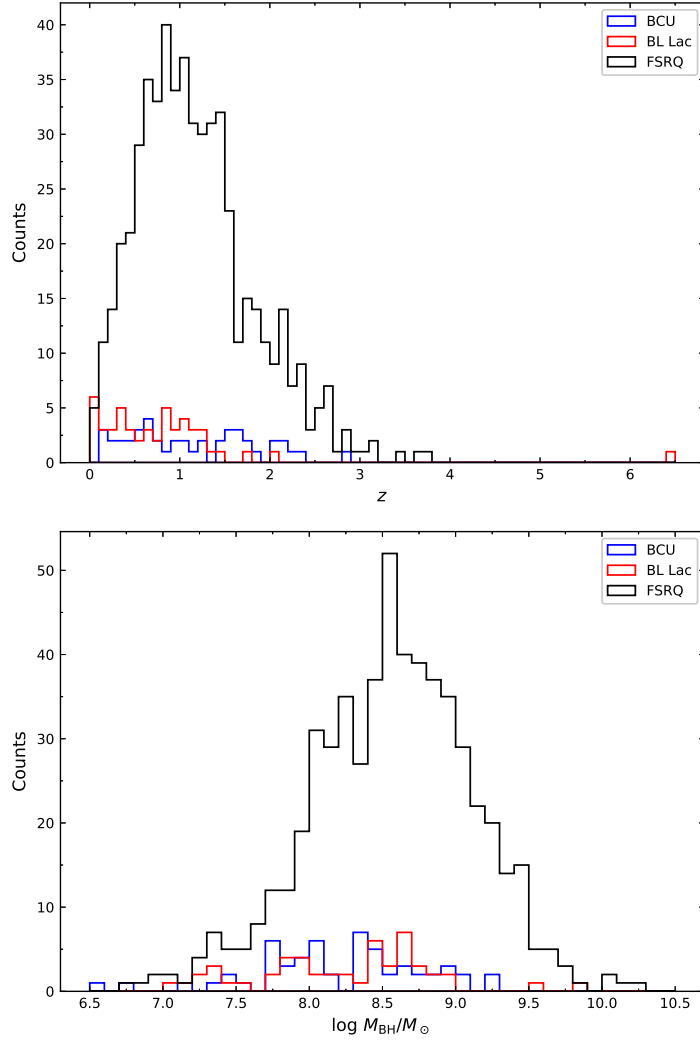


Figure 1. The distributions of redshift (upper panel) and BH mass (lower panel) for the blazars of this work. The blue histogram stands for BCU, the red one stands for BL Lac, and the black one stands for FSRQ, respectively.

3.3. The correlation between γ -ray luminosity and BLR luminosity

Fig. 3 shows BLR luminosity as a function of γ -ray luminosity. The OLS bisector regression is employed to find correlation between BLR luminosity and γ -ray luminosity, the result finds

$$\log L_{\text{BLR}} = (0.85 \pm 0.02)\log L_{\gamma} + (5.19 \pm 1.15),$$

Pearson partial analysis indicates a $r = 0.14$ and a $p = 5.7 \times 10^{-4}$ after removing the redshift effect from these two quantities. The result suggests that γ -ray luminosity is weakly correlated with BLR luminosity, although an apparently strong positive correlation is showing.

3.4. The correlation between γ -ray luminosity and jet radiation power: a lower-limit of Doppler factor

Fig. 4 shows jet radiation power as a function of γ -ray luminosity. During the analysis, we adopt the value of P_{rad} from Ghisellini et al. (2014) for the common sources. OLS bisector linear regression is employed to study the correlation between jet radiation power and γ -ray luminosity for the sources in our sample. The regression result gives

$$\log P_{\text{rad}} = (0.92 \pm 0.04)\log L_{\gamma} + (2.81 \pm 2.05),$$

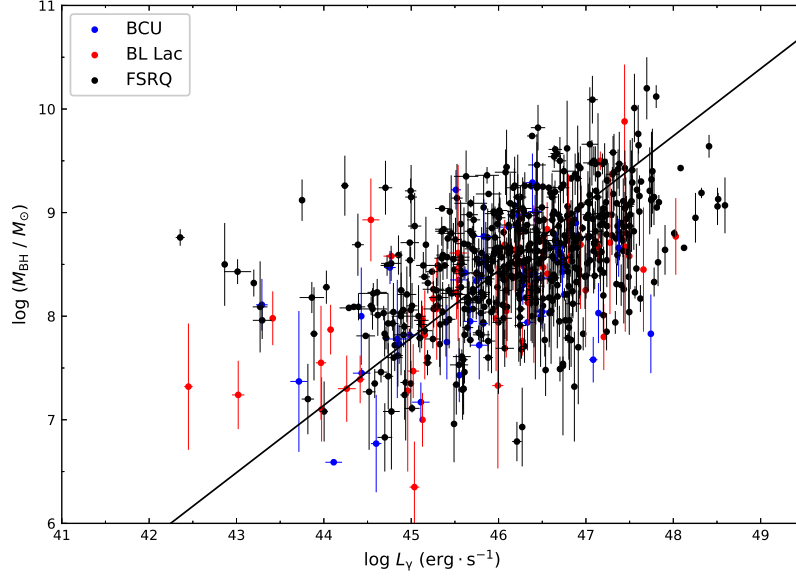


Figure 2. The correlation between BH mass and γ -ray luminosity. The black solid line stands for the result of linear regression. The blue dot stands for BCU, red dot stands for BL Lac, and black dot stands for FSRQ, respectively.

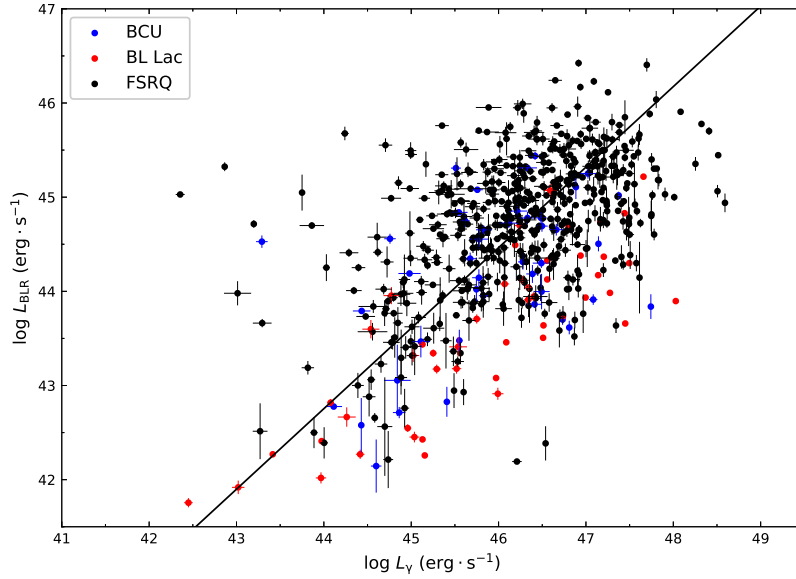


Figure 3. The correlation between BLR luminosity and γ -ray luminosity. The meaning of different symbols are as same as Fig. 2

with $r = 0.77$ and $p = 1.6 \times 10^{-38}$, which shows the jet radiation power is strongly correlated with γ -ray luminosity.

The blazar γ -ray emission predominates its radiation power. In fact, the L_γ should be less than both P_{rad} and $L_{\text{jet}}^{\text{bol}}$. However, there are 185 sources that lie below the equivalent line in Fig. 4, showing larger L_γ than P_{rad} . The excess of L_γ against P_{rad} suggests a significant Doppler beaming effect.

We estimate a lower-limit of Doppler beaming factor by taking two assumptions that (1) the observed γ -ray luminosity L_γ is a representative of $L_{\text{jet}}^{\text{bol}}$, and (2) δ equals to Γ for blazars (Zhang et al. 2020). Therefore, we have

$$\delta = \left(2f \frac{L_{\text{jet}}^{\text{bol}}}{P_{\text{rad}}} \right)^{1/2} > \left(2f \frac{L_\gamma}{P_{\text{rad}}} \right)^{1/2}.$$

The lower-limit Doppler factor (δ) of our sources ranges from 3.0 to 48.6, with mean values for BL Lacs and FSRQs being $\delta_{\text{BL Lac}} = 7.94 \pm 2.39$ and $\delta_{\text{FSRQ}} = 11.55 \pm 6.50$, the individual values are listed in column (10) of Table 2.

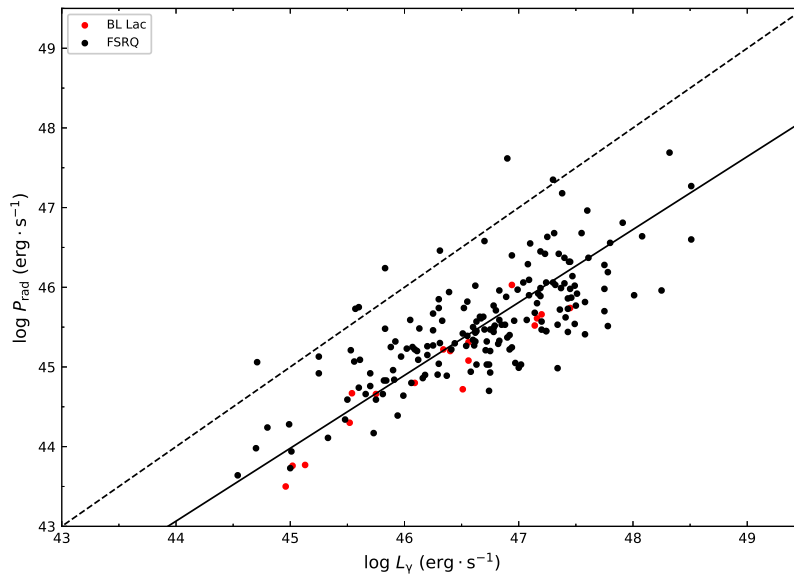


Figure 4. The correlation between jet radiation power and γ -ray luminosity. The meaning of different symbols are as same as Fig. 2. The solid black line is the linear regression, and the dashed one is the equivalent line.

4. DISCUSSION

4.1. The correlations

BH mass is one of the key ingredients of jet origination and radiation scenarios. There are many kinds of approaches to estimate the BH mass by using observable quantities, i.e., emission line luminosity, absorption line luminosity, stellar velocity dispersion, etc (Graham 2007; Gültekin et al. 2009; Shen et al. 2011; Shaw et al. 2012). In this work, we adopt BH mass that is estimated by using emission lines to avoid variance between different methods, we collect the BH mass information from Paliya et al. (2021). Fig. 1 show different distributions of both M_{BH} , because we have 10 times larger sample of FSRQs than BL Lacs. The average values indicate that FSRQs and BL Lacs have no significant difference in their BH masses, and this maybe caused by the limited number of BL Lacs in our sample. The predicted BH masses of BL Lacs should be averagely greater than the masses of FSRQs according to the presumed ‘blazar cosmic evolution’, in which the high-power ($L_{\text{bol}} > 10^{46}$ erg \cdot s $^{-1}$) blazars (mostly FSRQs) evolve to the low-power blazars (mainly BL Lacs). BH mass keeps growing by accretion during the evolution (Cavaliere & D’Elia 2002; Böttcher & Dermer 2002), even there are different opinions about it (Fan 2003).

The correlation between BH mass and γ -ray luminosity was studied by Soares & Nemmen (2020) through using a sample of 154 FSRQs, and they proposed that the M_{BH}/M_\odot is proportional to $L_\gamma^{0.37}$. In the present work, we have a larger sample and revisit this correlation. We have confirmed the positive and strong correlation between BH mass and γ -ray luminosity for blazars as shown in Fig. 2. Both Soares & Nemmen (2020)’s and our results suggest blazar with more massive BH tend to have stronger γ -ray emission and to have a more powerful jet, and the power of jet will be discussed in section 4.3. However, we have a larger slope, which is 0.65, and suggest M_{BH}/M_\odot proportional to $L_\gamma^{0.65}$ that indicates BH masses may grow faster with the γ -ray luminosity than they have predicted.

The correlation between L_γ and L_{BLR} has been performed in previous studies (Xiong & Zhang 2014; Zhang et al. 2019). This correlation proves that BLR provides seed photons for high energy γ -rays. More importantly, it would point towards a relation between the accretion rate and the jet power (Sbarrato et al. 2012) that we will discuss in the next section.

4.2. A new dividing line between FSRQs and BL Lacs

The correlation between the normalized γ -ray luminosity (L_γ/L_{Edd} , in Eddington units) and the normalized BLR luminosity ($L_{\text{BLR}}/L_{\text{Edd}}$) has been studied by Ghisellini et al. (2011) and Sbarrato et al. (2012).

$L_{\text{BLR}} = \xi L_{\text{Disk}}$ and $L_{\text{Disk}} = \eta \dot{M} c^2$, where ξ is photoionization coefficient, η is energy accretion efficiency, \dot{M} is an accretion rate; $L_{\text{Edd}} = \dot{M}_{\text{Edd}} c^2$, where \dot{M}_{Edd} is an Eddington accretion rate. Then we can get $\frac{L_{\text{BLR}}}{L_{\text{Edd}}} = \xi \eta \frac{\dot{M}}{\dot{M}_{\text{Edd}}}$ by substituting L_{BLR} and L_{Edd} . If one holds ξ and η to stay constant and assumes both of them to be 0.1 as former researchers did (Ghisellini et al. 2011; Sbarrato et al. 2012; Xiong & Zhang 2014). Thus, the separation is totally determined by the $\dot{M}/\dot{M}_{\text{Edd}}$, which was suggested to be 0.1 refer to $L_{\text{BLR}}/L_{\text{Edd}} = 1 \times 10^{-3}$ (Ghisellini et al. 2011). Later on, the value of $L_{\text{BLR}}/L_{\text{Edd}}$ was updated to be 5×10^{-4} (Sbarrato et al. 2012). The following study of Xiong & Zhang (2014) confirmed the idea of separation. They concluded the boundary of accretion ratio (in Eddington units) to be $\dot{M}/\dot{M}_{\text{Edd}} = 0.1$, with FSRQs showing $\dot{M}/\dot{M}_{\text{Edd}} > 0.1$ and BL Lacs showing $\dot{M}/\dot{M}_{\text{Edd}} < 0.1$.

While we must bear in mind that η and ξ are both assumed to be 0.1 in previous studies. Here, we test the assumptions that $\xi = 0.1$ and $\eta = 0.1$ before we study the separation for blazars. ξ can be calculated with L_{BLR} and L_{Disk} for 166 sources (16 BL Lacs and 150 FSRQs) in our sample. L_{BLR} is obtained through emission lines properties and L_{Disk} is obtained from Ghisellini et al. (2014), in which they preformed SED fitting to get the disk luminosity for blazars in their sample. The distribution of ξ is shown in Fig. 5, a mean $\mu = 0.11$ and standard deviation $\sigma = 0.05$ are obtained when a Gaussian fitting is employed to this distribution. The η is difficult to estimate because it couples with \dot{M} , which is not able to measure directly. A bolometric disk luminosity can be expressed as $L_{\text{Disk}} = \eta \dot{M} c^2$, which should less than L_{Edd} . Thus, we can estimate a lower-limit η because of $\eta \geq L_{\text{Disk}}/L_{\text{Edd}}$. The distribution of η lower-limit is shown in Fig. 6, and the distribution gives a mean $\mu = 0.05$ and standard deviation $\sigma = 0.09$ when a Gaussian fitting is adopted to the distribution. Our distributions of ξ and η suggest that the presumed values for both ξ and η are reasonable.

Ghisellini et al. (2011) and Sbarrato et al. (2012) obtained dividing lines to separate FSRQs and BL Lacs. It is interesting to revisit the dividing line using a larger sample. We draw our sample of blazars in Fig. 7 and notice many BL Lacs lying above the dividing lines that proposed by Ghisellini et al. (2011) and Sbarrato et al. (2012). Does that mean we need a new dividing line? In order to do this, we employ support vector machine (SVM), a kind of machine learning (ML) method, to accomplish the task of finding a new dividing line. The result of our dividing line gives an accuracy of 84.5% for the separation and is expressed as

$$\log \frac{L_{\text{BLR}}}{L_{\text{Edd}}} = 0.25 \log \frac{L_\gamma}{L_{\text{Edd}}} - 2.23.$$

The BL Lacs lying above the dividing line have larger accretion ratio than the BL Lacs below the line, and show consequently stronger emission from BLRs. According to the blazar evolution, we suggest these BL Lacs are at the early stage of the transition from FSRQs to BL Lacs. On the contrary, the FSRQs below the dividing line have smaller accretion ratio are at the late stage of transition. Moreover, we notice that there are sources, both in the above and below region, are located at the left region, $\log(L_\gamma/L_{\text{Edd}}) \lesssim -2$, of the diagram. These ‘left-region’ sources are likely to contain a broader jet and/or a misaligned jet and show the same emission-line luminosities with respect to blazars (Sbarrato et al. 2012). Abdo et al. (2010b) suggested that these ‘left-region’ sources maybe classified as radio galaxies rather than aligned blazars.

According to our result of the dividing line, we believe that $\dot{M}/\dot{M}_{\text{Edd}} = 0.1$ may not be a proper criteria to separate FSRQs and BL Lacs. Instead, we suggest $\dot{M}/\dot{M}_{\text{Edd}}$ evolve with the normalized γ -ray luminosity.

4.3. The central engine of jets

The origin of relativistic jets is still controversial. Blandford & Znajek (1977) (BZ) used a force-free approximation and perturbative approach to study the problem of jet formation by extracting BH rotation energy. With consideration of radiation pressure-dominated disk, one can obtain BZ-power as following

$$L_{\text{BZ}} \simeq L_{\text{Edd}} \frac{f_+^2(a) f_\Omega^2(a)}{4} \left(\frac{\beta_m}{\alpha} \right) \left(\frac{\dot{M} c^2}{L_{\text{Edd}}} \right)^{-3/2}, \quad (7)$$

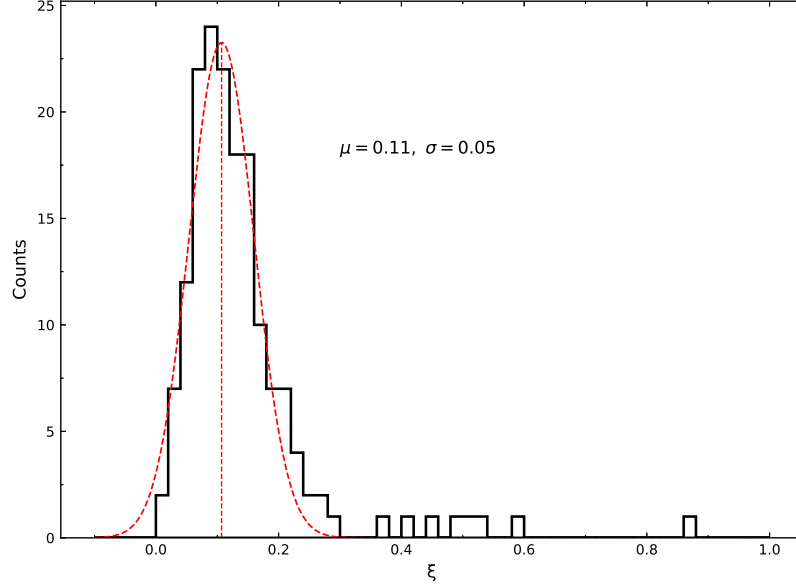


Figure 5. The distribution of ξ for the blazars. The dashed red curve stands for a Gaussian fitting of this distribution.

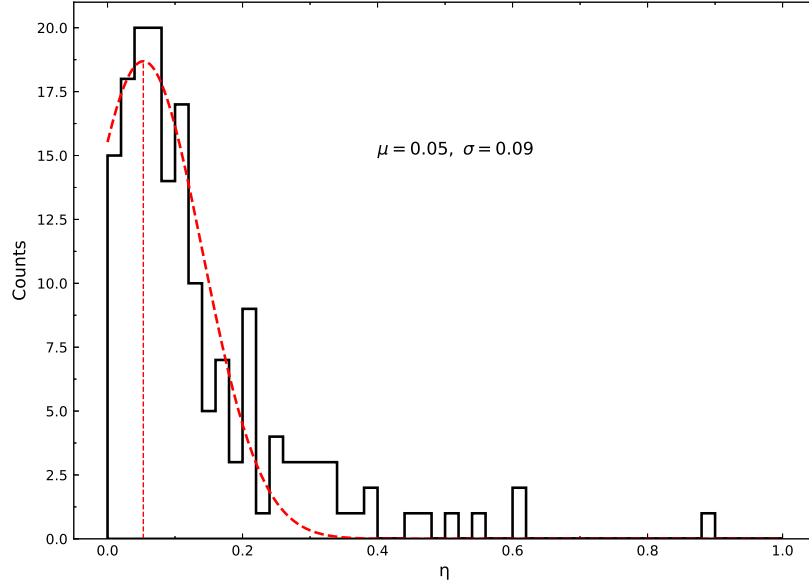


Figure 6. The distribution of η for the blazars. The dashed red curve stands for a Gaussian fitting of this distribution.

where \dot{M} is an accretion rate, $f_+(a)$ and $f_\Omega(a)$ are dimensionless quantities at order of 1, β_m is a proportion that the magnetic pressure as a fraction of the total thermodynamic disk pressure near the inner disk, and α gives the disk dissipation type (see Böttcher et al. 2012, Chap. 4.2). Assuming that the power through the Blandford-Znajek process to be entirely transformed into jets, the sum of jet kinetic power and jet radiation power, one can express jet power as

$$L_{\text{jet}} \simeq L_{\text{BZ}} \propto M_{\text{BH}} \cdot \left(\frac{L_{\text{Disk}}}{L_{\text{Edd}}} \right)^{-3/2}, \quad (8)$$

which suggests that a slope of 1.0 for $\log L_{\text{jet}}$ and $\log M_{\text{BH}}$ and a slope of $-3/2$ for $\log L_{\text{jet}}$ and $\log L_{\text{Disk}}/L_{\text{Edd}}$.

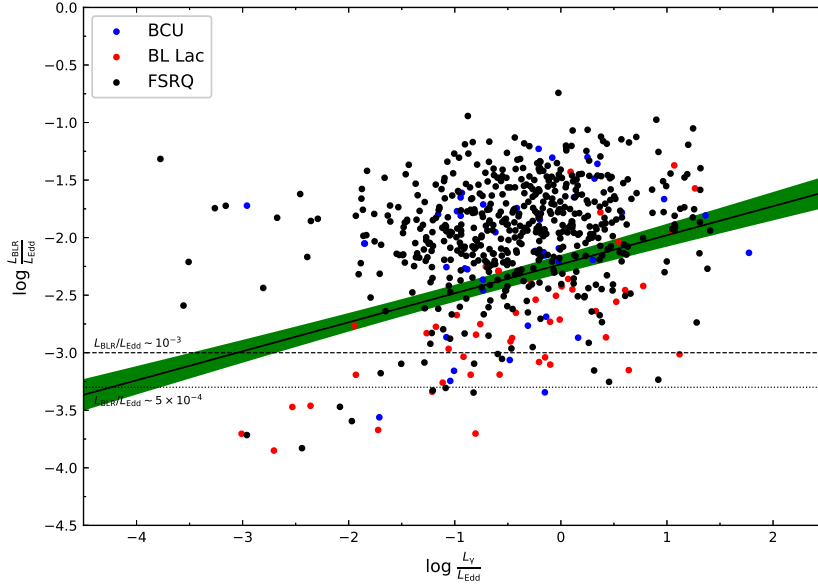


Figure 7. The correlation between normalized BLR luminosity and normalized γ -ray luminosity. The meaning of different symbols are as same as Fig2. The solid black dividing line is our best result from SVM, the green shade plot represents its 1σ error. The two horizontal lines indicate the divide between FSRQs and BL Lacs at $L_{\text{BLR}}/L_{\text{Edd}} \sim 10^{-3}$ from Ghisellini et al. (2011) (dashed) and at $L_{\text{BLR}}/L_{\text{Edd}} \sim 5 \times 10^{-4}$ from Sbarrato et al. (2012) (dotted).

In order to investigate the nature of jet power, we collect L_{Disk} , which estimated via modeling disk component with multi-temperature blackbody model in SED fitting procedure, from Ghisellini et al. (2014) and P_{jet} , which estimated via SED fitting, from Ghisellini et al. (2014) and Tan et al. (2020). When linear regressions are used for the correlation between the jet power and BH mass, significant correlations are obtained and shown in Fig. 8

$$\log P_{\text{jet}} = (1.16 \pm 0.15) \log \frac{M_{\text{BH}}}{M_{\odot}} + (36.52 \pm 1.24),$$

and $r = 0.59$ and $p = 0.02$ for BL Lacs; and

$$\log P_{\text{jet}} = (1.14 \pm 0.07) \log \frac{M_{\text{BH}}}{M_{\odot}} + (36.86 \pm 0.62),$$

and $r = 0.51$ and $p = 1.9 \times 10^{-11}$ for FSRQs. The results demonstrate strong correlations between the two quantities and suggest positive correlations between M_{BH} and L_{γ} for both BL Lacs and FSRQs. Moreover, slopes of 1.16 ± 0.15 and 1.14 ± 0.07 are consistent with the theoretically predicted slope that is 1.0 following Equation 8.

Fig. 9 shows the diagram of entire jet power P_{jet} against normalized disk luminosity $L_{\text{Disk}}/L_{\text{Edd}}$. It is found that there are 2 BL Lacs in red open circles, 4FGL J0407.5+0741 and 4FGL J0438.9-4521, that are marked as ‘1’ and ‘2’ respectively. 4FGL J0407.5+0741, known as TXS 0404+075, is a BL Lac class γ -ray emission object. However, this source is classified as FSRQs in other studies. Tan et al. (2020) suggested an external Compton model, which is usually applied to FSRQs due the existence of a BLR or a dust torus, to fit its broad band SED and studied the physical properties of FSRQs. Xiong & Zhang (2014) classified this source as a LSP, which is mostly consist of FSRQs, during their study of intrinsic γ -ray luminosity and jet power. This source shows typical a broad SED of FSRQ type, meanwhile, it shows the BL Lac optical spectrum. Therefore, the exact classification of this source is in debate, it is better to exclude this source when investigate the possible physical property difference between FSRQs and BL Lacs. 4FGL J0438.9-4521 has a redshift of 2.017 and a black hole mass of $\log(M_{\text{BH}}/M_{\odot}) = 7.8$. This black hole mass is relatively small with respect to the average values of the three classes in our sample. We notice that its BH mass was obtained according to the $C_{\text{IV}}(\lambda = 1549 \text{ \AA})$ emission line profile. However, the infrared emission could be significantly absorbed by the dust from the local to the galaxy itself, especially, the absorption from the latter one can hardly be measured and compensated. We believe that the mass of this source could be underestimated due to its lower

emission line luminosity of C_{IV} . We re-calculate the M_{BH} via the method that we have proposed in section 3.2 for 4FGL J0438.9-4521 and obtain a $\log(M_{BH}/M_{\odot}) = 9.23$. Then the plot is updated with a red dot marked as ‘2’ with an updated BH mass. Linear regressions are applied independently for BL Lacs and FSRQs

$$\log P_{jet} = -(1.77 \pm 0.40) \log \frac{L_{Disk}}{L_{Edd}} + (43.03 \pm 0.68),$$

with $r = -0.52$ and $p = 0.04$ for BL Lacs;

$$\log P_{jet} = (1.16 \pm 0.06) \log \frac{L_{Disk}}{L_{Edd}} + (47.89 \pm 0.62),$$

with $r = 0.27$ and $p = 8.5 \times 10^{-4}$ for FSRQs. The result of slope for BL Lac, -1.77 ± 0.40 , reaches the expected slope $-3/2$ following Equation 8, indicates jets are powered by extracting BH rotation energy for BL Lacs. A positive correlation with slope 1.16 for FSRQs suggests jets power comes from at least a mixture of extracting BH rotation power and disk accretion power, and the disk accretion power may be the dominant one.

The energy extraction from BH was well established by Blandford & Znajek (1977), and the following studies suggest that this process works in blazars and radio-loud narrow line Seyfert 1 AGNs (NLS1s) (Xiong & Zhang 2014; Foschini 2014). Xiong & Zhang (2014) studied the subject of blazar jet power through an investigation on the correlation between $\log L_{BLR}$ and $\log P_{jet}$ and obtained a slope 0.98 ± 0.07 for this correlation. Their results was perfectly consistent with the theoretically predicted slope 1 for $\log L_{BLR}$ vs $\log P_{jet}$, and suggested that *Fermi* blazars jets powered through the BZ mechanism.

In the present work, we have confirmed that the BZ mechanism makes great efforts in *Fermi* blazar jets powering. Moreover, our results seems to suggest BL Lacs maybe powered mostly by the BZ process that extracting energy from BH rotation. And the BL Lac jets are likely governed by the BH spin. While this result should be carefully used because we only have a small sample of 16 BL Lacs to study the correlation between these two quantities. For FSRQs, our results suggest that their jets are powered mostly by the accretion disk. And FSRQs jets raise from the inner region of accretion and the energy transformed through the magnetic field.

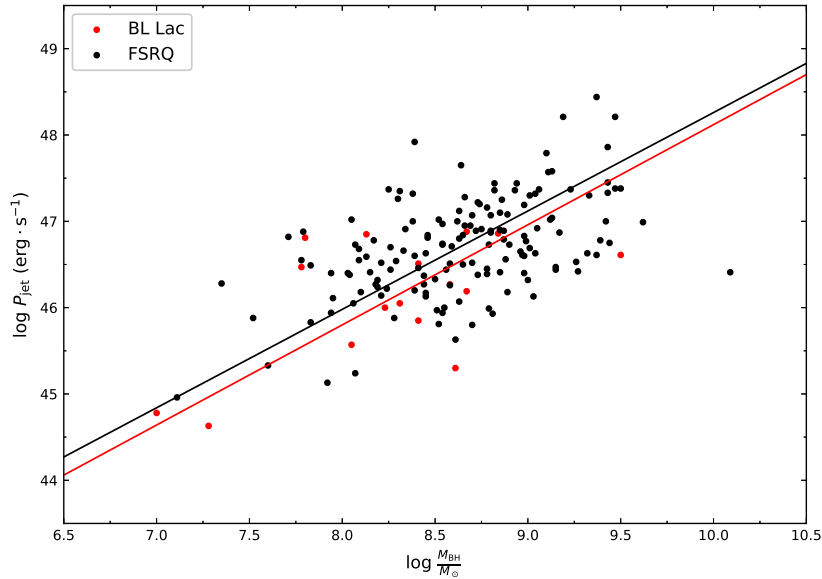


Figure 8. The correlation between entire jet power and BH mass. The meaning of different symbols are as same as Fig2.

4.4. Doppler beaming effect

Blazars are known to show extreme observation properties that are associated with the Doppler beaming effect. The beaming effect arises from the preferential orientation of the jet, typically within $< 20^\circ$ from our line of sight

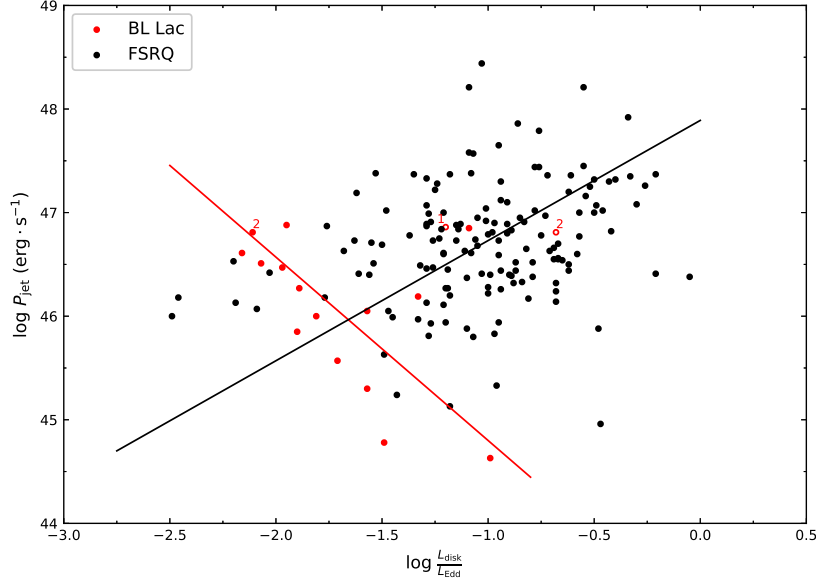


Figure 9. The correlation between entire jet power and disk luminosity divided by Eddington luminosity. The meaning of different symbols are as same as Fig2. The solid lines are represented for the linear regressions for FSRQs and BL Lacs. 4FGL J0407.5+0741 and 4FGL J0438.9-4521 are marked as ‘1’ and ‘2’.

(Readhead et al. 1978; Blandford & Königl 1979; Readhead 1980). This effect is quantified by a Doppler factor (δ), $\delta = [\Gamma(1 - \beta \cos\theta)]^{-1}$, where Γ is bulk Lorentz factor ($\Gamma = 1/\sqrt{1 - \beta^2}$), β is velocity of the jet in units of speed of light, and θ is the viewing angle. Since there is no direct way to measure β or θ , δ can only be estimated by indirect methods (Hovatta et al. 2009; Fan et al. 2013, 2014; Ghisellini et al. 2014; Chen 2018; Liodakis et al. 2018; Zhang et al. 2020). While different methods often yield discrepant results. Hovatta et al. (2009) and Liodakis et al. (2018) determined the variability Doppler factor at radio band by analyzing baazar light curves. However, the estimation at radio bands may not suitable for using in γ -ray bands. Because the γ -ray emission is extremely variable and γ -ray emission have different mechanisms, which are synchrotron-self Compton (SSC) process and external Compton (EC) process in the leptonic scenario, compare to the radio emission mechanism, which is the synchrotron process. Doppler factor estimation at γ -ray band was proposed by Zhang et al. (2020), δ^{Z20} can be calculated through L_γ and L_{BLR} for FSRQs and BL Lacs respectively, $\log \delta_{\text{FSRQ}}^{Z20} = (\log L_\gamma - 1.18 \log L_{\text{BLR}} + 8.00)^{0.5}$ and $\log \delta_{\text{BLLac}}^{Z20} = (\log L_\gamma + 0.87 \log L_{\text{BLR}} + 6.23)^{0.5}$.

In order to make comparisons with δ that we have calculated in section 3.4. We calculate γ -ray Doppler factor using Zhang et al. (2020)’s method for the sources in our sample, see as δ^{Z20} in Tab. 2 column (9). A Kolmogorov–Smirnov (K-S) test is applied to test if δ and δ^{Z20} are from the same distribution. The K-S test result gives $p = 1.8 \times 10^{-14}$ that indicates δ and δ^{Z20} are from two different distributions, and implies that the method we estimate δ is independent from Zhang et al. (2020)’s to estimate δ^{Z20} . δ^{Z20} ranges from in 1.31 to 202.31 with mean values of ($\langle \delta_{\text{FSRQ}}^{Z20} = 13.36$) and ($\langle \delta_{\text{BLLac}}^{Z20} = 11.02$). We suggest that δ and δ^{Z20} are comparable for two reasons (1) the average value of δ^{Z20} within the one σ error of δ , (2) the data points for the common sources are almost equally distributed below and above the equivalent line in the lower panel of Fig. 10. This result is expected because these two kinds of Doppler factors are both obtained at γ -ray band and both use γ -ray luminosity.

Besides, we collect Doppler factor from Liodakis et al. (2018), see as δ^{L18} in Tab. 2 column (8). Similarly, a K-S test with $p = 6.3 \times 10^{-10}$ suggests δ and δ^{L18} are from two different distributions, and implies that our method to estimate δ is independent from Liodakis et al. (2018)’s. δ^{L18} ranges from 1.11 to 88.44 with ($\langle \delta_{\text{FSRQ}}^{\text{L18}} = 22.46$) and ($\langle \delta_{\text{BLLac}}^{\text{L18}} = 20.97$).

Among δ , δ^{L18} and δ^{Z20} , δ^{L18} has the largest average values for both FSRQs and BL Lacs. δ^{L18} was driven from short term radio variability, while δ^{Z20} and δ are calculated through using 8-year γ -ray average flux, in which the rapid variability information had been washed out. One should keep in mind that a higher variability and shorter variability timescale yield a larger Doppler factor. Consequently, δ^{L18} has the largest average value among δ^{L18} , δ^{Z20} , and δ in this work.

Correlations between δ and δ^{Z20} , and δ^{L18} for 122 common sources are shown in Fig. 10. A correlation between $\log\delta$ and $\log\delta^{Z20}$ suggests our lower-limits of γ -ray Doppler factor is consistent with Zhang et al. (2020)'s, because we both estimate Doppler factors in the γ -ray band. However, our result is barely correlated with Liodakis et al. (2018)'s result due to different methods and wavelength bands that have been employed.

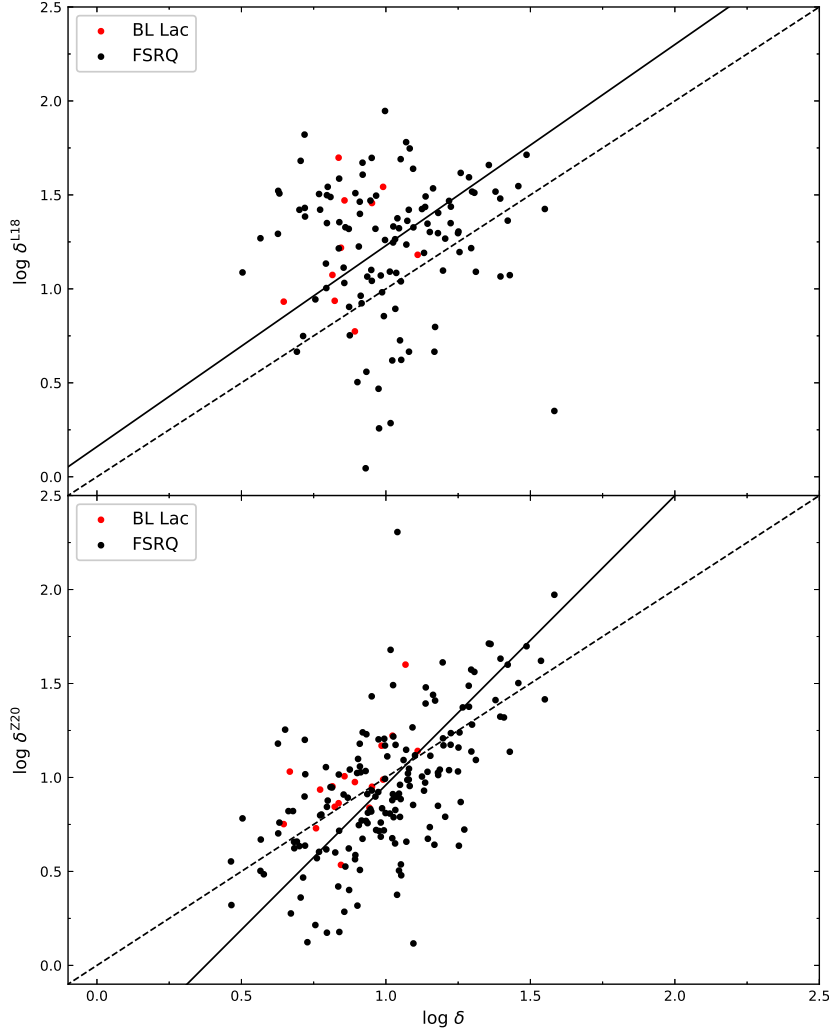


Figure 10. The comparison between the Doppler factor calculated in this work ($\log\delta$) and Doppler factors from Liodakis et al. (2018) ($\log\delta^{L18}$) and from Zhang et al. (2020) ($\log\delta^{Z20}$). The meaning of different symbols are as same as Fig. 2. The dashed lines are the corresponding equivalent lines.

5. CONCLUSION

In order to study blazar jet properties and its central engine, in this work, we have obtained a sample of 667 *Fermi* blazars that with available emission lines profiles, γ -ray emission and SED information from the literature. We have studied the correlations between γ -ray luminosity and BH mass, BLR luminosity and jet power, then further discussed accretion ratio separation of blazars, the jet origination, and proposed a new method of a lower-limit Doppler factor estimation.

Our main results are following: (1) The analysis between BH mass and the γ -ray luminosity show a strong correlation in logarithmic space. We propose a method to estimate the BH mass from γ -ray luminosity that expressed

as $M_{\text{BH}}/M_{\odot} \simeq L_{\gamma}^{0.65}/21.46$. (2) The correlation between BLR luminosity and γ -ray luminosity is weak. Then we normalize these two quantities with Eddington luminosity, and generate a dividing line to separate FSRQs and BL Lacs via the ML method. The dividing line is a symbol of the accretion ratio, we suggest the accretion ratio is evolved with normalized γ -ray luminosity. (3) Through the study between jet power and BH mass, and disk luminosity. We have confirmed that the BZ mechanism works in the BH-disk system of blazars. Specifically, the BL Lacs jets are likely powered mainly from extracting BH rotation energy while FSRQs jets are mostly powered by an accretion disk. (4) We propose a method of estimating a lower-limit of Doppler factor using L_{γ} and P_{rad} , give average values $\delta_{\text{FSRQ}} = 11.55 \pm 6.50$ and $\delta_{\text{BL Lac}} = 7.94 \pm 2.39$.

1 We thank the support from our laboratory, the key laboratory for astrophysics of Shanghai, and we thank Dr. Vaidehi
2 S. Paliya for sharing data and exchanging ideas of this work. Meanwhile, L. P. Fu acknowledges the support from the
3 National Natural Science Foundation of China (NSFC) grants 11933002, STCSM grants 18590780100, 19590780100,
4 SMEC Innovation Program 2019-01-07-00-02-E00032 and Shuguang Program 19SG41. S. H. Zhang acknowledges the
5 support from by Natural Science Foundation of Shanghai (20ZR1473600). J. H. Fan acknowledges the support by the
6 NSFC (NSFC 11733001, NSFC U2031201, NSFC U1531245).

Table 1. Optical and γ -ray parameters

4FGL name (1)	Class (2)	z (3)	F_{γ} (4)	Unc. F_{γ} (5)	Γ_{ph} (6)	$\log L_{\text{H}\alpha}$ (7)	$\log L_{\text{H}\beta}$ (8)	$\log L_{\text{MgII}}$ (9)	$\log L_{\text{CIV}}$ (10)	$\log M_{\text{BH}}/M_{\odot}$ (11)
J0001.5+2113	F	1.106	1.36E-09	6.86E-11	2.66	42.942 ± 0.016	42.029 ± 0.054	42.503 ± 0.032		7.54 ± 0.07
J0004.3+4614	F	1.81	2.41E-10	3.92E-11	2.58				44.126 ± 0.031	8.36 ± 0.1
J0004.4-4737	F	0.88	4.36E-10	3.75E-11	2.37			42.885 ± 0.099		8.28 ± 0.27
J0006.3-0620	B	0.346676	1.40E-10	3.13E-11	2.13	42.782 ± 0.189	42.004 ± 0.227			8.93 ± 0.4
J0010.6+2043	F	0.5978	1.73E-10	3.44E-11	2.32		43.047 ± 0.048	43.027 ± 0.017		7.86 ± 0.04

NOTE—Column definitions: (1) 4FGL name; (2) Classification, ‘B’ stands for BL Lacs, ‘F’ stands for FSRQs, ‘U’ stands for BCUs; (3) redshift; (4) integral photon flux from 1 to 100 GeV, in units of $\text{photon} \cdot \text{cm}^{-2} \cdot \text{s}^{-1}$; (5) 1σ error of F_{γ} ; (6) photon index; (7) luminosity of $\text{H}\alpha$ emission line, in units of $\text{erg} \cdot \text{cm}^{-1} \cdot \text{s}^{-1}$; (8) luminosity of $\text{H}\beta$ emission line in units of $\text{erg} \cdot \text{cm}^{-1} \cdot \text{s}^{-1}$; (9) luminosity of Mg II emission line in units of $\text{erg} \cdot \text{cm}^{-1} \cdot \text{s}^{-1}$; (10) luminosity of C IV emission line in units of $\text{erg} \cdot \text{cm}^{-1} \cdot \text{s}^{-1}$; (11) BH mass, in units of solar mass. Only 5 objects are presented here, the table is available in its entirety in machine-readable form.

Table 2. Jet parameters

4FGL name (1)	Class (2)	z (3)	$\log P_{\text{rad}}$ (4)	$\log P_{\text{jet}}$ (5)	$\log L_{\text{Disk}} \text{ (SED)}$ (6)	Ref. (7)	δ^{L18} (8)	δ^{Z20} (9)	δ (10)
J0001.5+2113	F	1.106						40.77	
J0004.3+4614	F	1.81					7.75	5.63	
J0004.4-4737	F	0.88	44.64	45.88	45.32	G14		10.50	11.92
J0006.3-0620	B	0.346676					6.96	2.48	
J0010.6+2043	F	0.5978					6.02	2.92	

NOTE—Column definitions: (1) 4FGL name; (2) Classification, ‘B’ stands for BL Lacs, ‘F’ stands for FSRQs, ‘U’ stands for BCUs; (3) redshift; (4) jet radiation power, in units of $\text{photon} \cdot \text{cm}^{-2} \cdot \text{s}^{-1}$; (5) jet entire power, in units of $\text{photon} \cdot \text{cm}^{-2} \cdot \text{s}^{-1}$; (6) luminosity of accretion disk, in units of $\text{erg} \cdot \text{cm}^{-1} \cdot \text{s}^{-1}$; (7) references of P_{rad} , P_{jet} , and L_{Disk} , that ‘G14’ stands for Ghisellini et al. (2014) and ‘T20’ stands for Tan et al. (2020); (8) Doppler factor from Lioudakis et al. (2018); (9) estimated Doppler factor using the method proposed in Zhang et al. (2020); (10) estimated lower-limit Doppler factor in the present work. Only 5 objects are presented here, the table is available in its entirety in machine-readable form.

REFERENCES

- Abdo, A. A., Ackermann, M., Agudo, I., et al. 2010a, ApJ, 716, 30, doi: [10.1088/0004-637X/716/1/30](https://doi.org/10.1088/0004-637X/716/1/30)
Abdo, A. A., Ackermann, M., Ajello, M., et al. 2010b, ApJ, 720, 912, doi: [10.1088/0004-637X/720/1/912](https://doi.org/10.1088/0004-637X/720/1/912)

- Abdollahi, S., Acero, F., Ackermann, M., et al. 2020, *ApJS*, 247, 33, doi: [10.3847/1538-4365/ab6bcb](https://doi.org/10.3847/1538-4365/ab6bcb)
- Baldwin, J. A., Wampler, E. J., & Burbidge, E. M. 1981, *ApJ*, 243, 76, doi: [10.1086/158568](https://doi.org/10.1086/158568)
- Blandford, R. D., & Königl, A. 1979, *ApJ*, 232, 34, doi: [10.1086/157262](https://doi.org/10.1086/157262)
- Blandford, R. D., & Payne, D. G. 1982, *MNRAS*, 199, 883, doi: [10.1093/mnras/199.4.883](https://doi.org/10.1093/mnras/199.4.883)
- Blandford, R. D., & Rees, M. J. 1978, *Pittsburgh Conference on BL Lac Objects*, 328
- Blandford, R. D., & Znajek, R. L. 1977, *MNRAS*, 179, 433, doi: [10.1093/mnras/179.3.433](https://doi.org/10.1093/mnras/179.3.433)
- Böttcher, M., & Dermer, C. D. 2002, *ApJ*, 564, 86, doi: [10.1086/324134](https://doi.org/10.1086/324134)
- Böttcher, M., Harris, D. E., & Krawczynski, H. 2012, *Relativistic Jets from Active Galactic Nuclei (WILEY-VCH Verlag GmbH & Co. KGaA)*
- Calderone, G., Ghisellini, G., Colpi, M., & Dotti, M. 2013, *MNRAS*, 431, 210, doi: [10.1093/mnras/stt157](https://doi.org/10.1093/mnras/stt157)
- Cavagnolo, K. W., McNamara, B. R., Nulsen, P. E. J., et al. 2010, *ApJ*, 720, 1066, doi: [10.1088/0004-637X/720/2/1066](https://doi.org/10.1088/0004-637X/720/2/1066)
- Cavaliere, A., & D'Elia, V. 2002, *ApJ*, 571, 226, doi: [10.1086/339778](https://doi.org/10.1086/339778)
- Celotti, A., Padovani, P., & Ghisellini, G. 1997, *MNRAS*, 286, 415, doi: [10.1093/mnras/286.2.415](https://doi.org/10.1093/mnras/286.2.415)
- Chen, L. 2018, *ApJS*, 235, 39, doi: [10.3847/1538-4365/aab8fb](https://doi.org/10.3847/1538-4365/aab8fb)
- Chen, Y. Y., Zhang, X., Zhang, H. J., & Yu, X. L. 2015, *MNRAS*, 451, 4193, doi: [10.1093/mnras/stv658](https://doi.org/10.1093/mnras/stv658)
- Fan, J.-H. 2002, *PASJ*, 54, L55, doi: [10.1093/pasj/54.4.L55](https://doi.org/10.1093/pasj/54.4.L55)
- Fan, J. H. 2003, *ApJL*, 585, L23, doi: [10.1086/374033](https://doi.org/10.1086/374033)
- Fan, J.-H., Bastieri, D., Yang, J.-H., et al. 2014, *Research in Astronomy and Astrophysics*, 14, 1135, doi: [10.1088/1674-4527/14/9/004](https://doi.org/10.1088/1674-4527/14/9/004)
- Fan, J.-H., Wang, Y.-J., Yang, J.-H., & Su, C.-Y. 2004, *ChJA&A*, 4, 533, doi: [10.1088/1009-9271/4/6/533](https://doi.org/10.1088/1009-9271/4/6/533)
- Fan, J.-H., Yang, J.-H., Liu, Y., & Zhang, J.-Y. 2013, *Research in Astronomy and Astrophysics*, 13, 259, doi: [10.1088/1674-4527/13/3/002](https://doi.org/10.1088/1674-4527/13/3/002)
- Fan, J. H., Yang, J. H., Liu, Y., et al. 2016, *ApJS*, 226, 20, doi: [10.3847/0067-0049/226/2/20](https://doi.org/10.3847/0067-0049/226/2/20)
- Fan, J. H., Yang, J. H., Xiao, H. B., et al. 2017, *ApJL*, 835, L38, doi: [10.3847/2041-8213/835/2/L38](https://doi.org/10.3847/2041-8213/835/2/L38)
- Foschini, L. 2014, in *International Journal of Modern Physics Conference Series*, Vol. 28, *International Journal of Modern Physics Conference Series*, 1460188, doi: [10.1142/S2010194514601884](https://doi.org/10.1142/S2010194514601884)
- Francis, P. J., Hewett, P. C., Foltz, C. B., et al. 1991, *ApJ*, 373, 465, doi: [10.1086/170066](https://doi.org/10.1086/170066)
- Ghisellini, G., & Tavecchio, F. 2010, *MNRAS*, 409, L79, doi: [10.1111/j.1745-3933.2010.00952.x](https://doi.org/10.1111/j.1745-3933.2010.00952.x)
- Ghisellini, G., Tavecchio, F., Foschini, L., & Ghirlanda, G. 2011, *MNRAS*, 414, 2674, doi: [10.1111/j.1365-2966.2011.18578.x](https://doi.org/10.1111/j.1365-2966.2011.18578.x)
- Ghisellini, G., Tavecchio, F., Maraschi, L., Celotti, A., & Sbarrato, T. 2014, *Nature*, 515, 376, doi: [10.1038/nature13856](https://doi.org/10.1038/nature13856)
- Graham, A. W. 2007, *MNRAS*, 379, 711, doi: [10.1111/j.1365-2966.2007.11950.x](https://doi.org/10.1111/j.1365-2966.2007.11950.x)
- Greene, J. E., & Ho, L. C. 2005, *ApJ*, 630, 122, doi: [10.1086/431897](https://doi.org/10.1086/431897)
- Gültekin, K., Richstone, D. O., Gebhardt, K., et al. 2009, *ApJ*, 698, 198, doi: [10.1088/0004-637X/698/1/198](https://doi.org/10.1088/0004-637X/698/1/198)
- Hovatta, T., Valtaoja, E., Tornikoski, M., & Lähteenmäki, A. 2009, *A&A*, 494, 527, doi: [10.1051/0004-6361:200811150](https://doi.org/10.1051/0004-6361:200811150)
- Kaspi, S., Maoz, D., Netzer, H., et al. 2005, *ApJ*, 629, 61, doi: [10.1086/431275](https://doi.org/10.1086/431275)
- Kaspi, S., Smith, P. S., Netzer, H., et al. 2000, *ApJ*, 533, 631, doi: [10.1086/308704](https://doi.org/10.1086/308704)
- Kellermann, K. I., Lister, M. L., Homan, D. C., et al. 2004, *ApJ*, 609, 539, doi: [10.1086/421289](https://doi.org/10.1086/421289)
- Lioudakis, I., Hovatta, T., Huppenkothen, D., et al. 2018, *ApJ*, 866, 137, doi: [10.3847/1538-4357/aae2b7](https://doi.org/10.3847/1538-4357/aae2b7)
- Lyutikov, M., & Kravchenko, E. V. 2017, *MNRAS*, 467, 3876, doi: [10.1093/mnras/stx359](https://doi.org/10.1093/mnras/stx359)
- McLure, R. J., & Dunlop, J. S. 2004, *MNRAS*, 352, 1390, doi: [10.1111/j.1365-2966.2004.08034.x](https://doi.org/10.1111/j.1365-2966.2004.08034.x)
- Nemmen, R. S., Georganopoulos, M., Guiriec, S., et al. 2012, *Science*, 338, 1445, doi: [10.1126/science.1227416](https://doi.org/10.1126/science.1227416)
- Paliya, V. S., Domínguez, A., Ajello, M., Olmo-García, A., & Hartmann, D. 2021, *ApJS*, 253, 46, doi: [10.3847/1538-4365/abe135](https://doi.org/10.3847/1538-4365/abe135)
- Pei, Z.-Y., Fan, J.-H., Liu, Y., et al. 2016, *Ap&SS*, 361, 237, doi: [10.1007/s10509-016-2822-0](https://doi.org/10.1007/s10509-016-2822-0)
- Rani, B., Krichbaum, T. P., Fuhrmann, L., et al. 2013, *A&A*, 552, A11, doi: [10.1051/0004-6361/201321058](https://doi.org/10.1051/0004-6361/201321058)
- Readhead, A. C. S. 1980, *PhysS*, 21, 662, doi: [10.1088/0031-8949/21/5/013](https://doi.org/10.1088/0031-8949/21/5/013)
- Readhead, A. C. S., Cohen, M. H., Pearson, T. J., & Wilkinson, P. N. 1978, *Nature*, 276, 768, doi: [10.1038/276768a0](https://doi.org/10.1038/276768a0)
- Sbarrato, T., Ghisellini, G., Maraschi, L., & Colpi, M. 2012, *MNRAS*, 421, 1764, doi: [10.1111/j.1365-2966.2012.20442.x](https://doi.org/10.1111/j.1365-2966.2012.20442.x)
- Scarpa, R., & Falomo, R. 1997, *A&A*, 325, 109
- Shaw, M. S., Romani, R. W., Cotter, G., et al. 2012, *ApJ*, 748, 49, doi: [10.1088/0004-637X/748/1/49](https://doi.org/10.1088/0004-637X/748/1/49)

- Shen, Y., Richards, G. T., Strauss, M. A., et al. 2011, *ApJS*, 194, 45, doi: [10.1088/0067-0049/194/2/45](https://doi.org/10.1088/0067-0049/194/2/45)
- Soares, G., & Nemmen, R. 2020, *MNRAS*, 495, 981, doi: [10.1093/mnras/staa1241](https://doi.org/10.1093/mnras/staa1241)
- Tan, C., Xue, R., Du, L.-M., et al. 2020, *ApJS*, 248, 27, doi: [10.3847/1538-4365/ab8cc6](https://doi.org/10.3847/1538-4365/ab8cc6)
- Urry, C. M., & Padovani, P. 1995, *PASP*, 107, 803, doi: [10.1086/133630](https://doi.org/10.1086/133630)
- Urry, C. M., Scarpa, R., O'Dowd, M., et al. 2000, *ApJ*, 532, 816, doi: [10.1086/308616](https://doi.org/10.1086/308616)
- Vestergaard, M., & Osmer, P. S. 2009, *ApJ*, 699, 800, doi: [10.1088/0004-637X/699/1/800](https://doi.org/10.1088/0004-637X/699/1/800)
- Vestergaard, M., & Peterson, B. M. 2006, *ApJ*, 641, 689, doi: [10.1086/500572](https://doi.org/10.1086/500572)
- Wandel, A., Peterson, B. M., & Malkan, M. A. 1999, *ApJ*, 526, 579, doi: [10.1086/308017](https://doi.org/10.1086/308017)
- Wills, B. J., Wills, D., Breger, M., Antonucci, R. R. J., & Barvainis, R. 1992, *ApJ*, 398, 454, doi: [10.1086/171869](https://doi.org/10.1086/171869)
- Woo, J.-H., & Urry, C. M. 2002, *ApJ*, 579, 530, doi: [10.1086/342878](https://doi.org/10.1086/342878)
- Xiao, H., Fan, J., Yang, J., et al. 2019, *Science China Physics, Mechanics, and Astronomy*, 62, 129811, doi: [10.1007/s11433-018-9371-x](https://doi.org/10.1007/s11433-018-9371-x)
- Xiao, H.-B., Pei, Z.-Y., Xie, H.-J., et al. 2015, *Ap&SS*, 359, 39, doi: [10.1007/s10509-015-2433-1](https://doi.org/10.1007/s10509-015-2433-1)
- Xiong, D. R., & Zhang, X. 2014, *MNRAS*, 441, 3375, doi: [10.1093/mnras/stu755](https://doi.org/10.1093/mnras/stu755)
- Zhang, L., Chen, S., Xiao, H., Cai, J., & Fan, J. 2020, *ApJ*, 897, 10, doi: [10.3847/1538-4357/ab9180](https://doi.org/10.3847/1538-4357/ab9180)
- Zhang, L., Fan, J., & Yuan, Y. 2019, arXiv e-prints, arXiv:1903.05849. <https://arxiv.org/abs/1903.05849>